HHS Public Access

Author manuscript

Drug Deliv Transl Res. Author manuscript; available in PMC 2019 April 01.

Published in final edited form as:

Drug Deliv Transl Res. 2018 April ; 8(2): 422–435. doi:10.1007/s13346-017-0435-y.

Nanoparticles in Thermosensitive Gel based Composite Nanosystem for Ocular Diseases

Vibhuti Agrahari[1], **Sulabh P. Patel**[1], **Nikhil Dhall**[2,*], **Zach Aulgur**[2,*], **Siddhant Thukral**[2,*], **Xiaoyan Yang**[1], **Ryan Conley**[3], and **Ashim K. Mitra**[1,§]

[1]Division of Pharmaceutical Sciences, School of Pharmacy, University of Missouri-Kansas City, Kansas City, MO 64108, USA

[2]School of Medicine, University of Missouri-Kansas City, Kansas City, MO 64108, USA

[3]Ira A. Fulton Schools of Engineering, Arizona State University, Tempe, AZ, 85281, USA

Abstract

The pentablock (PB) copolymers based composite nanosystems has been designed to provide a long-term delivery of macromolecules to the back of the eye. A unique arrangement of each block (polyethylene glycol, polylactic acid and polycaprolactone) with various molecular weights (PB-A and PB-B) was selected for the synthesis of nanoparticles (NPs) and thermosensitive gel (PB-C) by sequential ring-opening bulk copolymerization reaction. PB copolymers were characterized for their molecular weight and purity by ^{1}H-NMR spectroscopy and crystallinity by PXRD. The macromolecule model drugs [lysozyme (Lyz: ~14.5 kDa), IgG-Fab (~50 kDa) and IgG (~150 kDa)] were selected to delineate the effect of molecular weights on *in vitro* release profile of nanoformulations. Lyz, Fab and IgG encapsulated NPs were prepared by double emulsion solvent evaporation method. The entrapment efficiency (EE%) and drug loading (DL%) of macromolecules was higher for PB-B copolymers due to its higher molecular weight and hydrophobicity compare to PB-A. The particle size range of NPs was ~200–270 nm. *In vitro* release profiles of Lyz, Fab and IgG encapsulated in NPs alone and NPs suspended in gel (composite nanosystem) demonstrated a minimal burst release over a long period. The effect of hydrodynamic diameter of macromolecules and hydrophobicity of PB copolymers has been investigated on the release profile of nanosystems. *In vitro* biocompatibility study showed negligible cytokine (IL-1, IL-6 and TNF-α) release, which confirmed the safety of the PB copolymers. Based on the results, it is anticipated that long-term ocular delivery of macromolecules can be achieved through composite nanosystems developed in this study.

Graphical abstract

[§]Correspondence should be addressed to; **Ashim K. Mitra, Ph.D.**, University of Missouri Curators' Distinguished Professor of Pharmacy, Chair, Division of Pharmaceutical Sciences, University of Missouri-Kansas City, 2464 Charlotte Street, Kansas City, MO 64108, Phone: 816-235-1615; Fax: 816-235-5779, mitraa@umkc.edu.

[*]Authors contributed equally

CONFLICT OF INTEREST

I-Novion Inc., Genentech Inc.

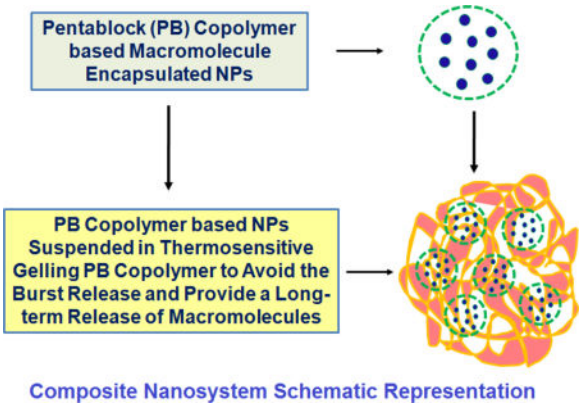

Keywords

Block copolymers; controlled and long-term release; intravitreal; macromolecule; posterior eye diseases; protein therapeutics

INTRODUCTION

The normal aging process of the eye is characterized by a continuous loss of photoreceptors (PRs), Bruch's membrane thickening, choroid thinning, scleral stiffening, vitreous degradation, and accumulation of debris. Among the posterior eye diseases; diabetic retinopathy, macular edema, and macular degeneration are the leading causes of age-related vision loss [1–2]. Macular degeneration occurs when a small area in the retina (macula) deteriorates. It is age related degenerative process, hence referred as age-related macular degeneration (AMD) and damages the retinal pigment epithelium (RPE) and PR [3]. With progression, AMD can be classified into the dry- and wet-forms based on the absence or presence of vascular growth progression from the choroidal side toward the retina. It is further subdivided into non-neovascular (NNV) (dry AMD) and neovascular (NV) (wet-AMD) AMD [4]. In wet-AMD, new blood vessels from the choroid may leak, resulting in macular edema. If left untreated, the progression may cause a centrally blinding disciform scar. Multiple factors such as angiogenesis, oxidative stress, lipid metabolism, and immune system activation play a key role in AMD pathogenesis [5].

Several factors are involved in ocular angiogenesis, with vascular endothelial growth factor (VEGF) playing a central role [6]. VEGF-A is a 46 kDa glycoprotein produced by ocular cells in response to oxidative stress and potent mediator of both retinal and choroidal angiogenesis [7–8]. It stimulates endothelial cell growth, promotes vascular permeability, and induces the dissociation of tight junction components. In wet-AMD, a high level of VEGF is present below the RPE cell layer and around PRs. VEGF inhibition via intraocular anti-VEGF to prevent the formation of new blood vessels represents the cornerstone of wet-AMD therapies [8]. Recombinant humanized anti-VEGF antibody and/or fragments [e.g. ranibizumab: Lucentis®; Genentech/Roche), pegaptanib (Macugen®), aflibercept (Eylea®; Regeneron Pharmaceuticals), and bevacizumab (off label drug: Avastin®; Genentech/Roche)], are Food and Drug Administration (FDA) approved therapies for wet-AMD [3].

However, the current treatments suffer from various challenges, including frequent intraocular injections, related side-effects, high cost of the therapy, and presence of several ocular barriers (anatomical and physiological) which significantly impaired the drug delivery to the posterior eye [9].

The application of nanotechnology has recently been shown improvements in ocular drug delivery and offers several treatment options [10]. Various FDA approved biodegradable polymers such as polycaprolactone (PCL), polylactic acid (PLA), polyglycolic acid (PGA) and polyethylene glycol (PEG) have been extensively investigated for controlled delivery of macromolecules as matrices of nanoparticles (NPs) [11–12]. Several investigators have applied block copolymers such as polylactide-co-glycolide (PLGA) [13], PEG-PLGA [14], PCL-PEG-PCL [15], for the development of controlled release formulation of large molecules/macromolecules/biologics (protein, peptide, antibody, Fab, Fc fragments). However, these polymers showed a burst drug release, which may cause toxicity and safety issues and restricts their further use [13, 18]. Moreover, a long-term macromolecule release has not been achieved. Hence, there is a critical need to develop a biocompatible polymeric system to provide a controlled and long-term release of macromolecule drugs in ocular therapeutics.

In order to achieve the above outcomes, various sequences of block copolymers can be tailor-made by considering physical chemical properties of FDA approved polymers. Among those, PEG provides hydrophilicity to copolymer which helps to degrade the matrix. PCL possesses crystallinity and hydrophobicity which enhances the drug entrapment efficiency. PLA and PGA are other polymers; those are more hydrophilic compared to PCL. These polymers contribute to rapid degradation of the matrix. Based on the tunable properties of these polymers, various tailor made combinations on the basis of different molecular weight, ratios and arrangements can be designed to achieve a particular release rate. Moreover, block copolymers are amphiphilic in nature, rendering these materials suitable for protein delivery.

Therefore, the objective of the current work is to synthesize copolymers of unique ratios and molecular weights consisting the PEG, PLA and PCL blocks for controlled and long-term delivery of macromolecules. The hypothesis of this project is centered on determining the effects of hydrophobicity and molecular weight of copolymers in NPs formulation, drug encapsulation efficiency, and the drug release profiling. To the best of our knowledge, this is the first investigation that has been performed to compare the effect of hydrodynamic diameter of macromolecules, polymer arrangements (various ratios and molecular weight), and hydrophobicity of polymers on the release profile of macromolecules. Furthermore, in order to minimize the burst release and to achieve a controlled long-term drug release profile, novel composite nanosystems comprising drug loaded NPs embedded in the thermosensitive gelling copolymer were designed (composite nanosystem schematic representation figure). The physicochemical characterization of nanoformulations in addition to the biocompatibility studies of copolymers has been performed to ensure their safety in ocular applications.

MATERIALS AND METHODS

Materials

Poly (ethylene glycol) (PEG, 4 kDa), methoxy-PEG (550 Da), stannous octoate, ε-caprolactone, poly (vinyl alcohol) (PVA), lipopolysaccharide, and *Micrococcus luteus* were procured from Sigma-Aldarich (St. Louis, MO). L-lactide and hexamethylenediisocynate (HMDI) were purchased from Acros organics (Morris Plains, NJ). Micro-BCA™ assay kit was obtained from Fisher scientific Inc., (Rockford, IL). Mouse tumor necrosis factor alpha (TNF-α), Interleukin 6 (IL-6), Interleukin 1 beta (IL-1β), and enzyme-linked immunosorbent assay (ELISA) kit were purchased from e-Bioscience Inc., (San Diego, CA). All other reagents used in this study were of analytical grade.

Methods

Synthesis of PB copolymers—PB copolymers i.e, poly(caprolactone)-poly(lactic acid)-poly(ethylene glycol)-poly(lactic acid)-poly(caprolactone) (PCL-PLA-PEG-PLA-PCL i.e., PB-A and PB-B) and poly(ethylene glycol)-poly(caprolactone)-poly(lactic acid)-poly(caprolactone)-poly(ethylene glycol) (PEG-PCL-PLA-PCL-PEG i.e., PB-C) were synthesized by two steps sequential ring-opening bulk copolymerization method [11–12]. The PB-A and PB-B copolymers were similar in block arrangements, but, have different molecular weights. PEG (4 kDa) and stannous octoate were used as macroinitiator and catalyst, respectively.

In the first step, triblock (TB) copolymers PLA-PEG-PLA (Figure 1, Step 1) of different molecular weights [(PLA_{3000}-PEG_{4000}-PLA3000 and PLA_{6000}-PEG_{4000}-PLA_{6000})] were synthesized by polymerization of PLA at two open hydroxyl ends of the PEG. Lactic acid and stannous octoate (0.5% w/w) were added to anhydrous PEG while the temperature was raised to 130°C. After 24 h, the reaction mixture was dissolved in dichloromethane (DCM) followed by precipitation in cold petroleum ether. The precipitated TB copolymer was filtered and dried overnight using high speed under vacuum at room temperature (Rotatory evaporator, BUCHI Labortechnik AG, Flawil, Switzerland). In the second step, PLA-PEG-PLA (TB) copolymers and ε-caprolactone were placed in a round bottom flask under the inert condition and temperature was raised to 130°C (Figure 1, Step 2). To this reaction mixture, stannous octoate (0.5% w/w) was added and the reaction was allowed to run for 24 h. Subsequently, PB copolymer (Table 1) was purified by the cold ether precipitation method as described in the first step. The final product was dried under vacuum and stored at −20°C until further use.

To synthesize the thermosensitive gelling copolymer (PB-C), TB copolymer ($mPEG_{550}$-PCL_{825}-PLA_{250}) was first synthesized by ring-opening bulk copolymerization as described earlier (Figure 2). The polymerization of ε-caprolactone was performed at the hydroxyl terminal of mPEG (550 Da) which was followed by another polymerization with L-lactide. The resulting TB copolymer was coupled with PLA using HMDI as a linker. The coupling reaction was carried out at 70°C for 8 h. The gelling copolymer was purified by cold ether precipitation followed by drying under vacuum and stored at −20°C (16).

Characterization of TB and PB copolymers

Proton nuclear magnetic resonance (^{1}H-NMR) spectroscopy: The synthesized copolymers were characterized for their molecular weight and purity by Proton Nuclear Magnetic Resonance (^{1}H-NMR) spectroscopy. The ^{1}H-NMR spectra of TB and PB copolymers were acquired on a 400 MHz NMR instrument (Varian Inc., Palo Alto, CA). The chemical shift *(δ)* values were reported as parts per million (ppm). NMR samples were prepared by dissolving each copolymer in deuterated chloroform in a 5-mm outer diameter NMR tubes (Wilmad-Lab Glass, Vineland, NJ).

Powder X-ray diffraction (PXRD) analysis: The crystallinity of copolymers was determined by PXRD analysis with Rigaku MiniFlex automated X-ray diffractometer (Rigaku, The Woodland, TX). The instrument was equipped with Ni-filtered Cu-Kα radiation (30 kV and 15 mA). The analysis was performed at room temperature at the scanning rate of 5°/min.

Phase transition (gelation) study of thermosensitive gelling copolymer (PB-C): The sol-gel transition behavior of PB-C gelling copolymer was examined by the test tube inverting method [11]. Briefly, the copolymer was dissolved in phosphate buffer saline (PBS, pH 7.4) at various concentrations ranging from 10–30 wt% and incubated for 12 h at 4°C. Afterwards, 1 ml of PB-C copolymer solution was placed in a 4 ml glass vial and put in a water bath. The temperature of the bath was raised slowly from 10 to 60°C at the rate of 1°C increment/min. The gel formation was observed visually by inverting the glass vials. A physical state of flow was characterized as sol-phase, whereas, a state of no flow was considered as the gel-phase.

In vitro biocompatibility studies—Mouse macrophage cells (RAW-264.7) were maintained according to the American Type Culture Collection (ATCC) guidelines at 37°C, 5% CO_2 and 95% humidified atmosphere for 48 h. The PB copolymers (PB-A, PB-B, and PB-C) were dissolved in acetonitrile at the concentration of 25 mg/ml. Two hundred microliters of this solution were aliquoted in 48-well cell culture plates and incubated for overnight under UV lights (laminar flow). The process continued with the acetonitrile evaporation and sterilization of resulting polymer film. After the sterilization, RAW-264.7 cells (5.0×10^4) were seeded in each well of the cell culture plate and incubated for 24 h at 37°C and 5% CO_2. After completion of the incubation period, cell supernatants were analyzed for the presence of TNF-α, IL-6, and IL-1β cytokines. Lipopolysaccharide (LPS) was selected as positive control, whereas, cells without any treatment were considered as negative control. Cytokines levels (in pg/ml) were measured by ELISA method according to the manufacturer's protocol (e-Biosciences, San Diego, CA). Standard calibration curves for TNF-α, IL-6 and IL-1β were prepared in the concentration ranges of 10–750 pg/ml, 5–500 pg/ml and 10–500 pg/ml, respectively, [11].

Formulation of PB NPs—Lyz, Fab and IgG-encapsulated NPs were prepared by water in oil in water ($W_1/O/W_2$) double emulsion solvent evaporation method using PB-A and PB-B copolymers [11–12]. Briefly, Fab containing aqueous solution (W_1 phase) was emulsified in the organic phase (dichloromethane: DCM) comprising PB-A or PB-B copolymer by drop-

wise addition to the aqueous phase containing 2% w/v polyvinyl alcohol (PVA). This was subjected to probe sonication for 30 sec at 2W output to form a W_1/O primary emulsion. The resulting primary emulsion was then added drop-wise to 5 ml of 2% w/v PVA solution (W_2 phase) under constant sonication for 60 sec at 2W output to prepare a $W_1/O/W_2$ double emulsion. To avoid the excessive heating and any possible degradation of macromolecule, emulsion preparation was carried out in ice-bath. The double emulsion was stirred at room temperature for 30 min followed by evaporation of DCM under vacuum using a rotatory evaporator to formulate the NPs. The emulsion containing NPs was centrifuged for 30 min at 20,000 rpm and 4°C followed by two washing cycles with distilled deionized water (DDW). The Lyz-loaded PB-A based NPs and IgG loaded PB-B based NPs were formulated according to the similar protocol. Finally, the Lyz, Fab and IgG-loaded NPs were freeze-dried in the presence of 5% w/w mannitol (as a cryoprotectant) and stored at −20°C until further use.

Physicochemical characterization of NPs

Particle size and polydispersity index (PDI): Freeze-dried NPs were dispersed in DDW at the concentration of 1 mg/ml and analyzed for particle size distribution using the Zetasizer (Zetasizer Nano ZS, Malvern Instruments Ltd, Worcestershire, UK) at 90° scattering angle. The NPs samples were analyzed in triplicate (n = 3).

Percent entrapment efficiency (EE %) and drug loading (DL %): Lyz, Fab and IgG encapsulated freeze-dried NPs were examined for their entrapment EE and DL by estimating the amount of protein in the supernatant obtained from NPs preparation. Micro BCA™ protein estimation kit was employed for the estimation of total protein. The samples were analyzed by a DTX 800 Multimode microplate reader (Beckman Coulter, Brea, CA). The standard curves of respective macromolecules (Lyz, Fab and IgG) ranging from 3.125 to 200 μg/ml were prepared in DDW. The following equations 1 and 2 were applied for the calculation of EE (%) and DL (%).

$$\mathrm{EE}(\%)=\frac{(\text{Initial amount of drug}-\text{Amount of drug in supernatan t})}{\text{Initial amount of drug}}\times 100 \quad \ldots\text{Eq.1}$$

$$\mathrm{DL}(\%)=\frac{\text{Amount of drug in NPs}}{\text{Total amount of drug and polymer}}\times 100 \quad \ldots\text{Eq.2}$$

In vitro drug release studies—The PB copolymer based NPs were characterized for their ability to release the Lyz, Fab and IgG from native NPs and NPs suspended in thermosensitive gelling copolymer (composite nanosystem). In order to conduct the *in vitro* drug release studies, 1 mg of each of Lyz, Fab and IgG equivalent freeze-dried NPs was suspended in 1 ml of Phosphate Buffer Saline (PBS; pH 7.4). The resulting NP suspension was then incubated in a water bath equilibrated at 37°C. At predefined time intervals, the suspension was centrifuged at 12,000 rpm for 30 min. Two hundred microliters of

supernatant was collected and replaced with the same volume of PBS. NPs were then resuspended and the release study was continued at 37°C. In a second set (composite nanosystem) of *in vitro* release studies, 1 mg equivalent of Lyz, Fab and IgG containing NPs was suspended in 100 μl of an aqueous solution of thermosensitive gelling copolymer (PB-C; 15 wt%). The resulting suspension was incubated in an Eppendorf tube at 37°C for 30 min. Once the gel was formed, an aliquot (1 ml) of PBS (pre-incubated at 37°C) was slowly added. At predetermined time intervals, 200 μl of supernatant was collected and replaced with the same volume of fresh PBS (pre-incubated at 37°C). The drug release samples were analyzed by Micro BCA™ assay for total protein content according to the supplier's instructions (Fisher scientific, Rockford, IL). *In vitro* release experiments were performed in triplicate (n = 3) and expressed as percent cumulative drug release with time.

In vitro drug release kinetics—In order to delineate the release kinetics mechanisms of Lyz, Fab and IgG from NPs and composite nanosystem, release data were fitted to first-order, Higuchi, Hixon Crowell, and Korsmeyer-Peppas models as given by Eqs. (3), (4), (5), and (6), respectively.

$$\log Q_t = \log Q_0 + \mathrm{K_1 t}/2.303 \quad \ldots \text{Eq.3}$$

$$Q_t = \mathrm{K_H} t^{0.5} \quad \ldots \text{Eq.4}$$

$$(\mathrm{Q_0}^{1/3} - \mathrm{Q_t}^{1/3} = \mathrm{K_{hc} t}) \quad \ldots \text{Eq.5}$$

$$\mathrm{Q_t}/\mathrm{Q_\infty} = \mathrm{kt^n} \quad \ldots \text{Eq.6}$$

In these Equations, Q_t is the amount of drug released at time *t*, Q_0 is the initial amount of drug in solution, K_1 is first order release constant, K_H is the Higuchi release rate constant, K_{hc} is Hixon Crowell release rate constant, Q_t/Q_∞ is the fraction of drug released at time *t*, Q_∞ is the total amount of drug released, and *k* is a kinetic constant. The constant *n* is the release exponent explaining the drug release mechanisms and classified as Fickian diffusion ($n \leq 0.5$), case-II transport ($n = 1$), anomalous transport ($0.5 < n < 1$), and super case-II transport ($n > 1$) [17].

Estimation of enzymatic activity of Lyz—The enzymatic activity of Lyz in the released samples was estimated by comparing with freshly prepared Lyz solutions and/or control samples. The controls were prepared with Lyz solution incubated at 37°C in PBS (pH 7.4). These solutions were parallel to the *in vitro* release study from composite nanosystem. In order to determine the enzymatic activity of Lyz, a stock solution of

Micrococcus luteus (0.01% w/v) was prepared with phosphate buffer (66 mM, pH 6.15) and diluted to achieve the absorbance between 0.2 – 0.6 at 450 nm. One hundred microliters of samples, standards, and controls were mixed with 2.5 ml of *Micrococcus luteus* suspension. The absorbance was measured at 450 nm over a period of 4 min at room temperature. Data were plotted for absorbance against time and slope was calculated to quantify the amount of Lyz in enzyme unit (EU). The EU units of Lyz (active) per mg of protein were calculated from the following equations 7 and 8 [18].

$$\text{Units of Lyz in one ml of sample} = \frac{(\Delta \text{A } 450\text{nm/ min Test} - \Delta \text{A } 450\text{nm/ min Blank})(df)}{(0.001)(0.1)} \quad \ldots \text{Eq.7}$$

$$\frac{\text{Units of Lyz}}{\text{mg of sample}} = \frac{\text{Units of Lyz in one ml of sample}}{\text{mg of Lyz in one ml sample}} \quad \ldots \text{Eq.8}$$

As per the definition of Lyz, one EU of enzyme is able to produce ΔAbs450nm of 0.001 per minute at pH 6.15 and 25°C utilizing *Micrococcus luteus* suspension. The number 0.1 represented the volume of release samples, standards, or controls and *df* depicts the dilution factor. The biological activity observed for the release samples were compared with the respective controls at the same time points.

Statistical analysis: The number of samples in each analysis is three and +/− in the results showed the standard deviation. The value of standard deviation is ≤ 2 which was under the acceptable range.

RESULTS AND DISCUSSION

Synthesis and characterization of copolymers

Synthesis of TB and PB copolymers—The PB-A, PB-B and PB-C copolymers were successfully synthesized by ring-opening bulk copolymerization of ε-caprolactone, and L-lactide. In the first step, TB copolymers were synthesized, purified and characterized as described in the method section. The resulting TB-A and TB-B copolymers were composed of a PEG central block bearing two PLA sequences at both ends. The purified TB-A, TB-B, and TB-C copolymers were then utilized for the synthesis of respective PB copolymers as depicted in Figures 1 and 2, respectively.

Characterization of TB and PB copolymers

^{1}H-NMR spectroscopy: The purity and molecular weights (Mn: number average molecular weight) of copolymers were calculated by ^{1}H-NMR spectroscopy. As shown in Figure 3A, the typical ^{1}H-NMR spectrum of PB-A showed peaks at 1.40, 1.65, 2.30 and 4.06 ppm

representing the methylene (− CH_2−) protons of − $(CH_2)_5$−, −OCO−CH_2−, and −CH_2OOC− of PCL units, respectively, (Figure 3A). Typical signals at 1.50 (−CH_3) and 5.17 (−CH) ppm were assigned to the PLA blocks. Figure 3B represented the ^{1}H-NMR spectrum of PB-C thermosensitive gelling copolymer. The peaks a, b and c were assigned as −CH_2− protons of the PCL block, while peaks e and f represented the −CH_3 and −CH− groups of the PLA block, respectively. The ratio of mPEG and ε-caprolactone was computed through the proton integration ratio of −CH_2− proton peak at 3.65 (d) and 2.3 (c), respectively, whereas for L-lactide it has been computed through –CH− proton peak at 5.10 (f). The molecular weights (Mn) of PB copolymers were similar to their theoretical molecular weights (Table 1). In this study, the theoretical molecular weights of copolymers were mentioned instead of their calculated molecular weights.

PXRD analysis: Interestingly, TB-1 and TB-2 (PLA-PEG-PLA) copolymers exhibited crystalline peaks at 2θ = 16°, 19°, and 23°, but, in PB-A and PB-B, the crystalline peaks of PCL were shifted to 2θ = 20.5° and 2θ = 21.5° as represented in Figures 4A and 4B, respectively. PXRD patterns of TB-A and TB-B indicated that PLA blocks retained their semi-crystalline structure, even after the covalent conjugation with the PCL blocks. Conjugation of PCL blocks at the terminals of TB-A and TB-B copolymers exhibited a shift in the intensity of the crystalline peak showing the semi-crystalline structures of PB-A and PB-B copolymers. Thus, the crystallinity of copolymers was easily controlled by the arrangement of the polymer blocks in their structural backbone. PB-C (Figure 4C) copolymer was devoid of any crystalline peak suggesting its amorphous nature. A previously published report suggested that a decrease in crystallinity enhanced the degradation of block copolymers which is anticipated from thermosensitive gelling copolymer [19].

Phase transition (gelation) of PB-C thermosensitive gelling copolymer: The thermosensitive gelling copolymers were amphiphilic in nature, containing hydrophilic block (PEG) and hydrophobic block(s) of PCL and/or PLA. The aqueous solution of PB-C was observed clear due to the self-assembly of polymeric chains into micellar structure which showed aggregation upon increasing the temperature and resulted in the gel formation. However, upper gel-sol conversion was due to an increased molecular motion of the hydrophobic chain of PCL and PLA. The aqueous solution of PB copolymers exhibited a sol-gel transition response upon increasing the temperature in the concentration range of 10–30% wt/wt. The transition temperature was found to be a function of copolymer concentrations. The phase diagram shown in Figure 5 revealed the critical gel concentration (CGC) from the solution to gel state conversion at 37°C. This physicochemical property makes these copolymers suitable for drug delivery applications.

In vitro biocompatibility studies of copolymers—The release of various cytokines releases such as TNF-α, IL-6 and IL-1β in culture supernatant following 24 h exposure to PB-A, PB-B and PB-C copolymers were examined. The samples were analyzed via sandwich ELISA method. Results depicted in Figure 6 indicated the release of TNF-α (~200 pg/ml) in both groups, i.e., PB-A, PB-B and PB-C. However, the values were comparable to the negative control (cells without treatment) with no significant differences. Similarly, a negligible release of IL-6 and IL-1β was observed, suggesting that these

copolymers are safe for use. These synthesized polymers did not induce any immune responses to the RAW 264.7 cells at higher than the working concentrations. Therefore, PB copolymers used in this study are considered as biocompatible and safe for further studies.

Formulation and characterization of copolymer based NPs

Formulation of NPs: The Lyz, Fab and IgG encapsulated PB copolymers based NPs were successfully prepared by $W_1/O/W_2$ double emulsion solvent evaporation method.

Particle size and PDI: The particle size of NPs was observed in the range of 200–260 nm (Table 2). A unimodal size distribution with a narrow PDI of (<0.5) of NPs was observed. These results suggested that the hydrodynamic diameter of macromolecules had no significant effect on the particle size distribution of NPs.

EE% and DL% evaluation: As presented in Table 2, the EE of Lyz, and Fab in PB-A NPs were ~42% and ~45% w/w, respectively. The low EE of NPs is probably due to the high hydrophilicity of macromolecules escaping from primary emulsion phase during the NPs synthesis to the large volume of the external phase. However, NPs prepared from PB-B copolymer exhibited a slightly higher EE ~49% w/w for Fab compared to PB-A NPs. This could be due to the reason that the high hydrophobicity of PB-B copolymer relative to PB-A may have produced a rapid polymer precipitation to form the NPs during the solvent evaporation step and provided a slightly higher EE (12). It is also plausible that EE and DL were affected by the increased ratio of lactide during the NP preparation. The hydrophobic segment of PLA-PCL chain and the hydrophilic drug were associated with the PEG core which reduced the escape to the outer aqueous phase. Also, the EE and DL of IgG (molecular weight ~150 kDa) encapsulated in PB-B NPs was calculated to determine the effect of molecular weight in EE and DL of PB copolymers. Results showed that due to the high molecular weight and hydrophobicity of PB-B, it was able to encapsulate (~51% w/w) the high molecular weight macromolecule (Table 2). Overall, the application of high molecular weight of PB copolymers ensured a higher EE and DL of large molecules encapsulated in NPs.

In vitro drug release studies: *In vitro* release profile of different molecular weight of macromolecules Lyz (~14.5 kDa), Fab (~50 kDa) and IgG (~150 kDa) were evaluated for; (A) PB-A and PB-B based NPs and (B) PB-A and PB-B NPs embedded in 15 wt% thermosensitive gelling copolymer (PB-C). The PB-A NPs formulations of Lyz and Fab demonstrated a biphasic release profile, i.e., initial burst release followed by a sustained release as shown in Figure 7A and 7B, respectively. Lyz and Fab exhibited the burst release of ~21% and ~19%, respectively, from PB-A NPs due to the presence of surface adsorbed drug. An approximately 80% drug release from PB-A NPs was observed for Lyz and Fab in ~13 and ~35 days, respectively. Hence, to eliminate and/or minimize the burst release effect and to and offer a long-term drug release profile throughout the release period, hydrogels have been utilized in the formulation development.

Lyz and Fab encapsulated PB-A NPs were suspended in the aqueous solution of thermosensitive gelling polymer (PB-C) termed as composite nanosystem. The aqueous

solution of PB-C copolymer remains in the liquid state at room temperature, but, immediately transitioned from solution to hydrogel at the physiological temperature of 37°C (sol-gel transition mechanism) entrapping NPs throughout the polymeric matrix. About 80% cumulative release of Lyz was observed from composite nanosystem for ~27 days compared to ~13 days in PB-A NPs (Figures 7A). Moreover, a prolonged release of Fab was observed as analyzed up to ~49 days from PB-A NPs (Figure 7B). This was due to the reason that NPs suspended into the gel matrix provided an additional diffusion barrier to the surface adsorbed drug. It also led to a sustained and long-term release pattern of the encapsulated drug throughout the release period [11], [16]. The effect of the molecular weights of the PB copolymers (PB-A and PB-B) on the release of Fab has been studied. Composite nanosystems of Fab (PB-A and PB-B NPs embedded in gelling copolymer) demonstrated a long-term sustained release profile as depicted in Figure 8A. Although PB-A copolymer promised a longer release profile relative to PB-B, but, composite nanosystem of PB-B showed a faster drug release profile compared to the PB-A copolymer. It might be due to the higher drug loading in PB-B NPs owing to the higher molecular weight and reduced crystallinity of PB-B compared to the PB-A copolymer.

The *In vitro* release profile of NPs formulations of Fab (Figure 8B) and IgG (Figure 9A) showed similar profiles as discussed above. The results showed that Fab exhibited a higher burst release (~21 %) relative to IgG (~18%) from the NPs alone. Similarly, composite nanosystems minimized the burst release (~ 10 %) and (~ 8 %) of Fab and IgG as shown in Figures 8B and 9A, respectively. The IgG composite nanosystem sustained its release for more than 8 weeks with high molecular weight PB-B. The *in vitro* release profiles of Lyz and Fab from PB-A copolymer and Fab and IgG from PB-B copolymer based formulations suggested that the hydrodynamic diameter of macromolecules exerted its effect on drug release as depicted in Figure 9B and 10A, respectively. The results suggested a higher burst release and shorter release duration for Fab relative to IgG from their respective NPs. Lyz has a smaller hydrodynamic diameter compared to Fab which probably led to its rapid diffusion through the polymeric matrices of NPs and composite nanosystem. The comparative release profiles of composite nanosystems studied in this study was represented in Figure 10B.

In vitro drug release kinetics—In order to evaluate the release mechanisms of NPs, *in vitro* drug release data were fitted in First-order, Higuchi, Hixson-Crowell, and Korsmeyer-Peppas kinetic models. Results presented in Table 3 indicated that Korsmeyer-Peppas was the best fit model for all the formulations with R^2 values ranging between 0.985–0.998. Moreover, n values in Korsmeyer-Peppas model for the release of Lyz, Fab and IgG from NPs were below 0.40 indicating the diffusion controlled release pattern. Interestingly, n values for composite nanosystem (NPs suspended in thermossensitive gel) of Lyz (0.402), Fab from PB-A (0.549), Fab from PB-B (0.582) and IgG (0.541) were suggested an anomalous diffusion controlled release mechanism. Hence, the release of macromolecules from composite nanosystem was controlled by diffusion as well as degradation of copolymer.

Enzymatic activity of Lyz in the released samples—The biological activity of Lyz in the released samples taken at different time points was displayed in Table 4. It was observed that the enzyme activity in the released samples diminished with time due to the reason that macromolecules remained in the release medium for a long time interval. In addition, hydrophobic residues caused the protein adsorption on polymer surface that resulted in the loss of biological activity of the entrapped protein. A decrease in enzymatic activity can be attributed to storage conditions which may not be the expected case under *in vivo* conditions. It is anticipated that during the NP preparation ($W_1/O/W_2$ double emulsion), PEG (hydrophilic block) may have oriented at aqueous-organic interface. Hence, PEG may have reduced the interaction of Lyz with the hydrophobic polymer segments (PCL and PLA) which avoided the denaturation of large molecules. Therefore, it was concluded that enzyme activity of the entrapped Lyz was lower due to longer exposure in the release medium.

CONCLUSION

The presented study discussed the synthesis and characterization of PB copolymers for the preparation of the composite nanosystem to achieve a controlled and long-term drug release profile of macromolecules. In order to eliminate the burst release phase, a novel composite nanosystem comprised of Lyz, Fab and IgG-encapsulated PB-A and/or PB-B NPs suspended in PB-C thermosensitive gel was successfully formulated. It was observed that the hydrodynamic diameter of macromolecules exerted its effects on drug release. The peppas model was the best fit model, suggesting that the release rate was controlled by diffusion and degradation of copolymers.

Results confirmed that the PB copolymer based composite delivery system are able to minimize the side effects associated with repeated every month intravitreal injections by lowering the injection frequency. In addition, the synthesized PB copolymers are biocompatible in nature and can be considered excellent biomaterials for ocular delivery. The enzyme activity of Lyz was observed up to three weeks. The integrity or stability of the protein molecule was not addressed in this work and an assessment of the compatibility of the polymers with the macromolecule remains to be elucidated in the future studies. However, the nanoformulations were optimized to achieve a high drug loading. This was essential so that a small volume of intravitreal injection containing a higher dose can be injected. This was also targeted in order to achieve a long-term delivery up to 3–6 months with an amount release of 2–10 μg/day. Overall, the outcomes from this study clearly suggested that the PB copolymers based control drug delivery system may serve as a promising platform not only for the back of the eye complications but also for the treatment of anterior segment eye diseases.

Acknowledgments

This study was supported by the award number R01 EY09171-14 from the National Institutes of Health (NIH). Authors are thankful to Dr. Anil Kumar (Division of Pharmacology and Toxicology, UMKC) for providing the UV-Plate Reader facility, Dr. James Murochiwick (Department of Geosciences, UMKC) for helping in PXRD analyses, Dr. Kun Cheng for allowing us to use the freeze-dryer, and Dr. Bi-Botti C. Youan (Division of Pharmaceutical Sciences, UMKC) for allowing us to use the Zetasizer Nano ZS instrument. Also, we are thankful to the School of

Graduate Studies (SGS), UMKC Research Grant and Graduate Assistant Fund (GAF), UMKC women's Council for providing the financial support.

References

1. Kang-Mieler JJ, Osswald CR, Mieler WF. Advances in ocular drug delivery: emphasis on the posterior segment. Expert opin on drug deliv. 2014; 11(10):1647–60.
2. Delplace V, Payne S, Shoichet M. Delivery strategies for treatment of age-related ocular diseases: From a biological understanding to biomaterial solutions. J of control release. 2015; 219:652–68. [PubMed: 26435454]
3. Agrahari V, Agrahari V, Mandal A, Pal D, Mitra AK. How are we improving the delivery to back of the eye? Advances and challenges of novel therapeutic approaches. Expert opin on drug deliv. 2016:1–17.
4. Jager RD, Mieler WF, Miller JW. Age-related macular degeneration. N Engl J med. 2008; 358(24): 2606–17. [PubMed: 18550876]
5. Shaw PX, Stiles T, Douglas C, Ho D, Fan W, Du H, et al. Oxidative stress, innate immunity, and age-related macular degeneration. AIMS mol sci. 2016; 3(2):196–221. [PubMed: 27239555]
6. Smith AG, Kaiser PK. Emerging treatments for wet age-related macular degeneration. Expert opin on emerg drugs. 2014; 19(1):157–64.
7. Park YG, Rhu HW, Kang S, Roh YJ. New Approach of Anti-VEGF Agents for Age-Related Macular Degeneration. J of ophthal. 2012; 2012:637316. [PubMed: 22496964]
8. Ozkiris A. Anti-VEGF agents for age-related macular degeneration. Expert opin on ther pat. 2010; 20(1):103–18.
9. Agrahari V, Mandal A, Agrahari V, Trinh HM, Joseph M, Ray A, et al. A comprehensive insight on ocular pharmacokinetics. Drug deliv and transl res. 2016; 6(6):735–54. [PubMed: 27798766]
10. Agrahari V, Agrahari V, Mitra AK. Nanocarrier fabrication and macromolecule drug delivery: challenges and opportunities. Ther deliv. 2016; 7(4):257–78. [PubMed: 27010987]
11. Agrahari V, Agrahari V, Hung WT, Christenson LK, Mitra AK. Composite Nanoformulation Therapeutics for Long-Term Ocular Delivery of Macromolecules. Mol pharm. 2016; 13(9):2912–22. [PubMed: 26828415]
12. Patel SP, Vaishya R, Patel A, Agrahari V, Pal D, Mitra AK. Optimization of novel pentablock copolymer based composite formulation for sustained delivery of peptide/protein in the treatment of ocular diseases. J of microencapsul. 2016; 33(2):103–13. [PubMed: 26964498]
13. Fonte P, Araujo F, Seabra V, Reis S, van de Weert M, Sarmento B. Co-encapsulation of lyoprotectants improves the stability of protein-loaded PLGA nanoparticles upon lyophilization. Int J of pharm. 2015; 496(2):850–62. [PubMed: 26474964]
14. Karve S, Werner ME, Cummings ND, Sukumar R, Wang EC, Zhang YA, et al. Formulation of diblock polymeric nanoparticles through nanoprecipitation technique. J of vis exp : JoVE. 2011; (55)
15. Gou M, Gong C, Zhang J, Wang X, Wang X, Gu Y, et al. Polymeric matrix for drug delivery: honokiol-loaded PCL-PEG-PCL nanoparticles in PEG-PCL-PEG thermosensitive hydrogel. J of biomed mat res Part A. 2010; 93(1):219–26.
16. Patel SP, Vaishya R, Yang X, Pal D, Mitra AK. Novel thermosensitive pentablock copolymers for sustained delivery of proteins in the treatment of posterior segment diseases. Protein and pept lett. 2014; 21(11):1185–200.
17. Yang X, Shah SJ, Wang Z, Agrahari V, Pal D, Mitra AK. Nanoparticle-based topical ophthalmic formulation for sustained release of stereoisomeric dipeptide prodrugs of ganciclovir. Drug deliv. 2016; 23(7):2399–409. [PubMed: 25564964]
18. Tang Y, Singh J. Biodegradable and biocompatible thermosensitive polymer based injectable implant for controlled release of protein. Int J of pharm. 2009; 365(1–2):34–43. [PubMed: 18786623]
19. Lam CX, Savalani MM, Teoh SH, Hutmacher DW. Dynamics of in vitro polymer degradation of polycaprolactone-based scaffolds: accelerated versus simulated physiological conditions. Biomed mat. 2008; 3(3):034108.

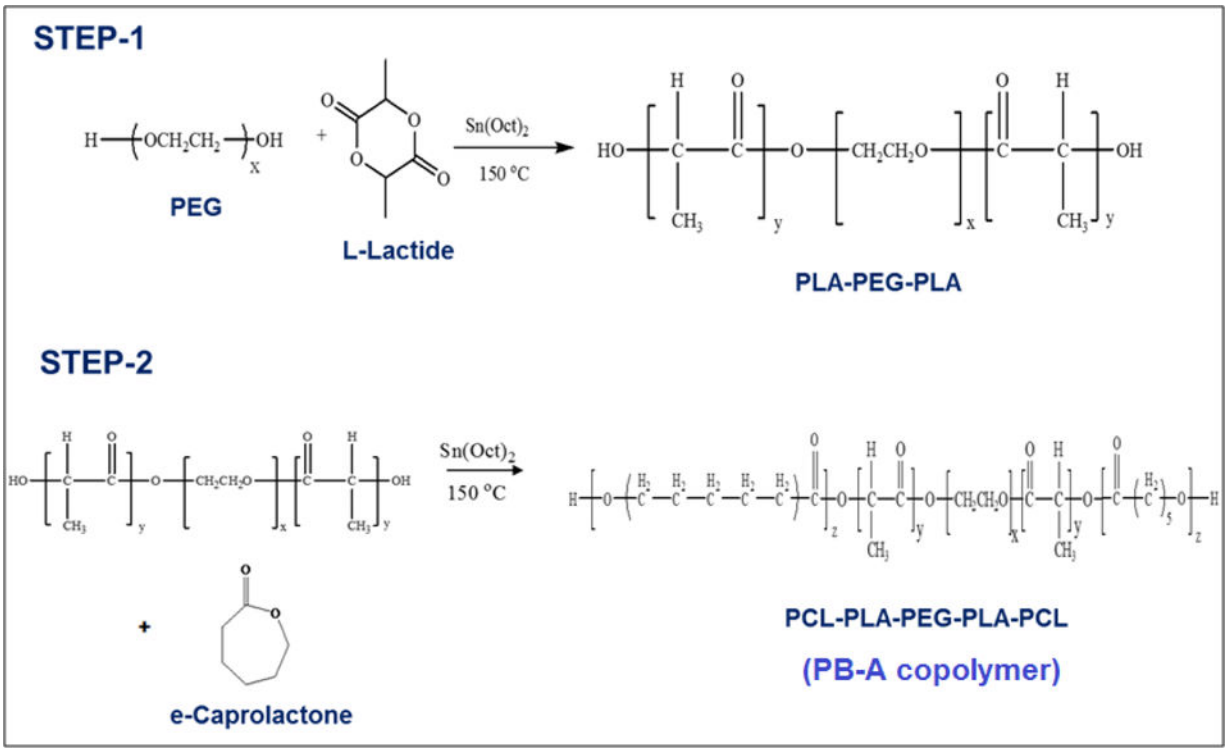

Figure 1.
Synthesis scheme for PB-A and PB-B (PCL-PLA-PEG-PLA-PCL) copolymer

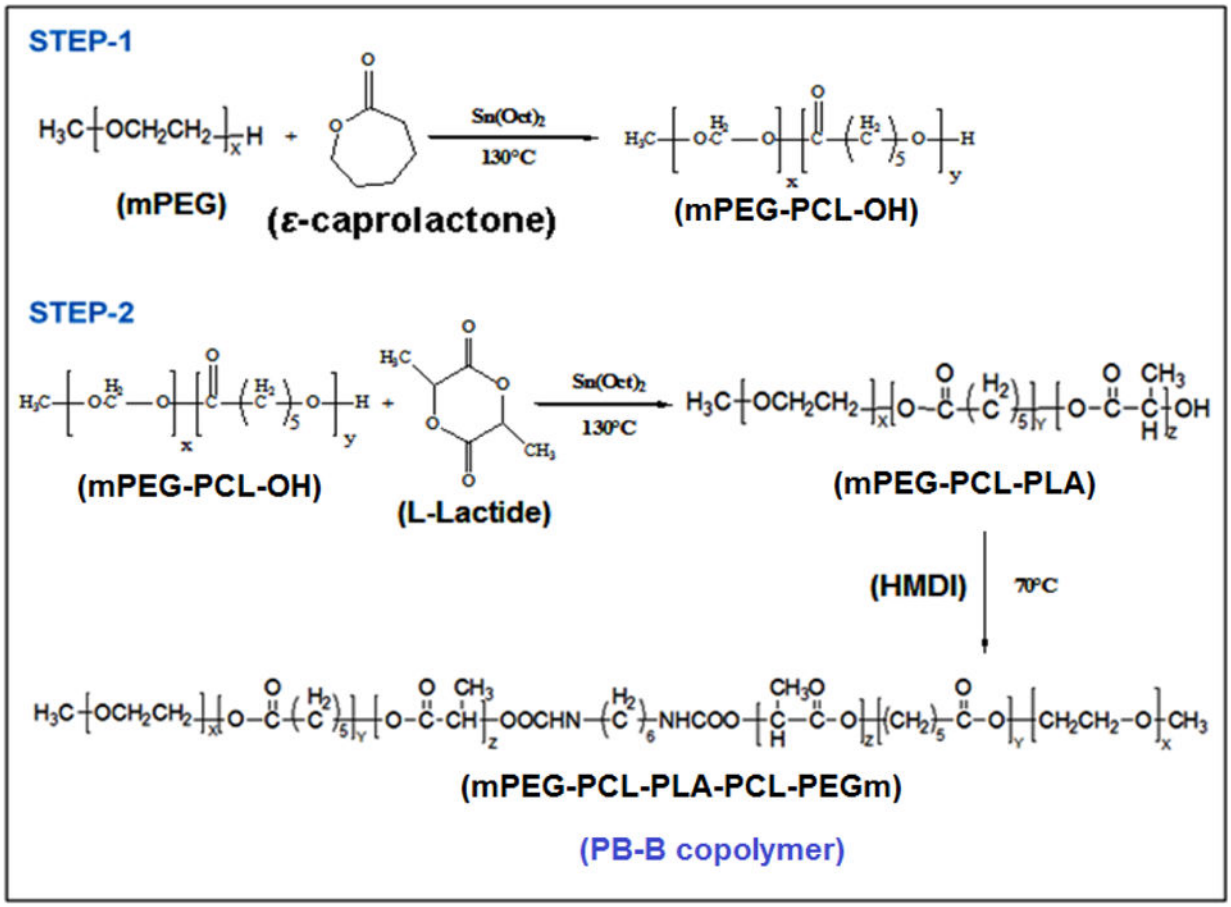

Figure 2.
Synthesis scheme for PB-C (PEG-PCL-PLA-PCL-PEG) copolymer (Reproduced with permision from Ref. 11)

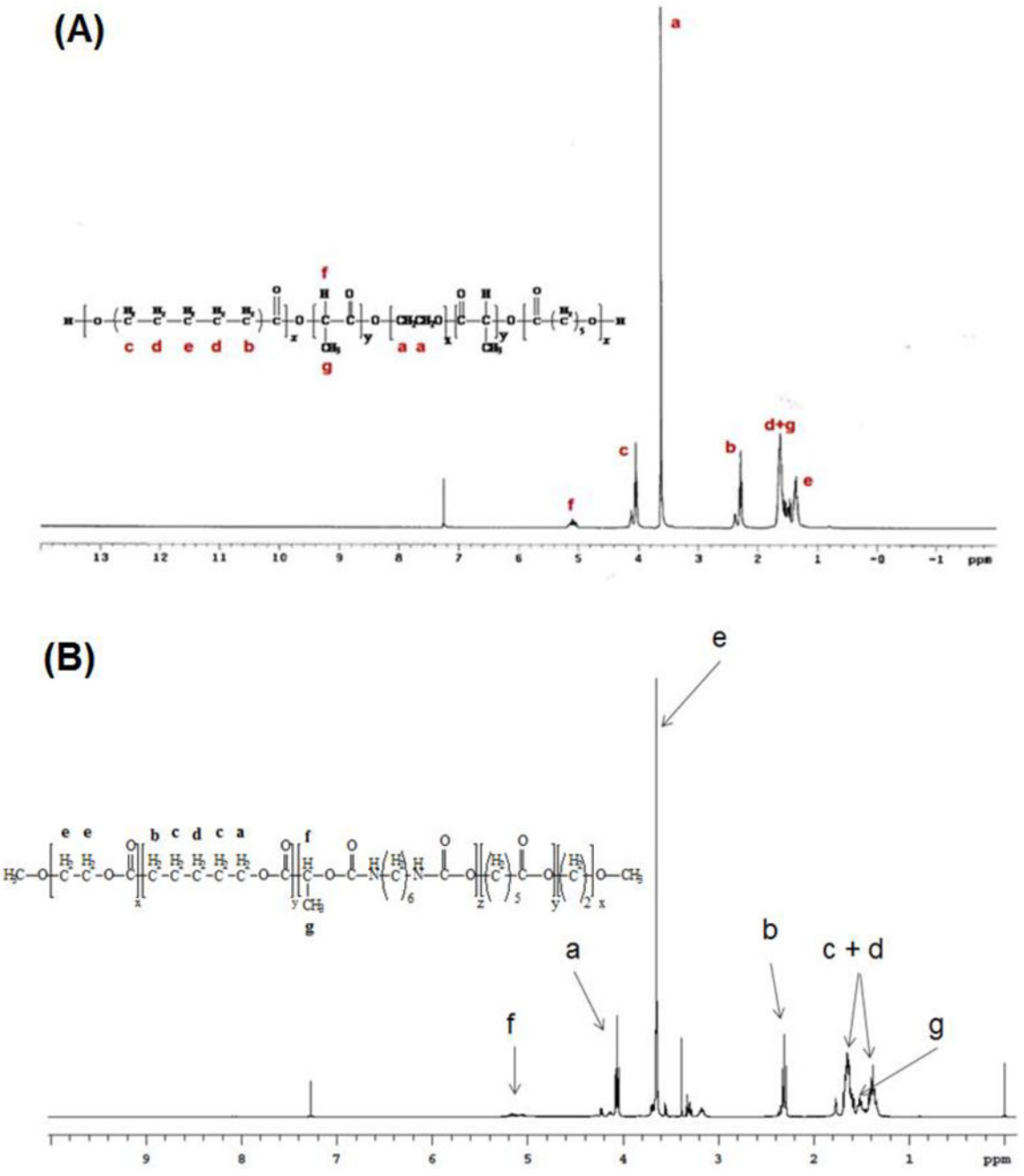

Figure 3.

(A) ^{1}H-Nuclear Magnetic Resonance (^{1}H-NMR) spectrogram of (A) PB-A, and (B) PB-C copolymer in $CDCl_3$ (NMR spectra of PB-C is modified with permission from Ref. 11)

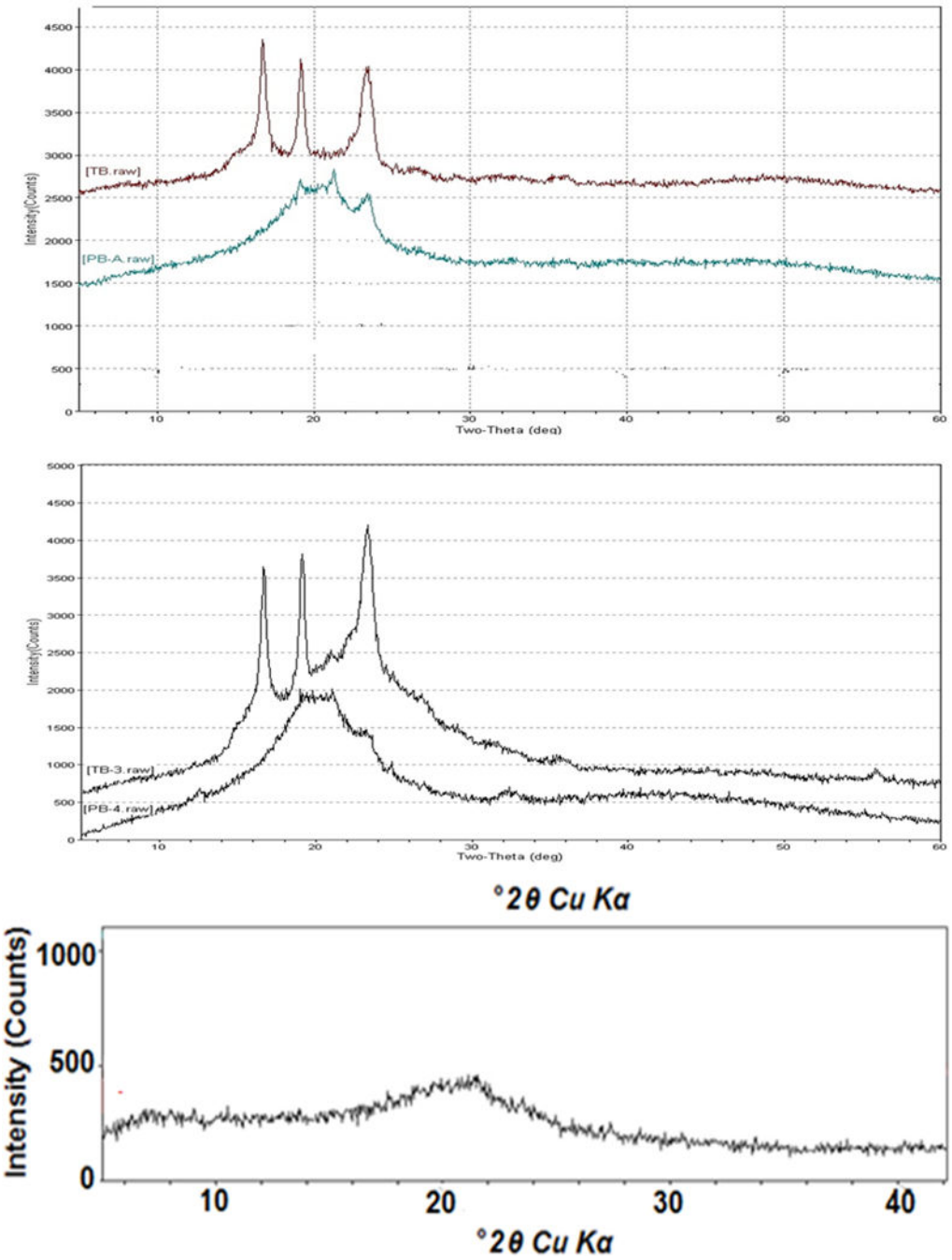

Figure 4.

Powder X-Ray Diffraction Analysis of (A) TB-A and PB-A (B) TB-B and PB-B (C) PB-C; (PB-C is reproduced with permision from Ref. 11)

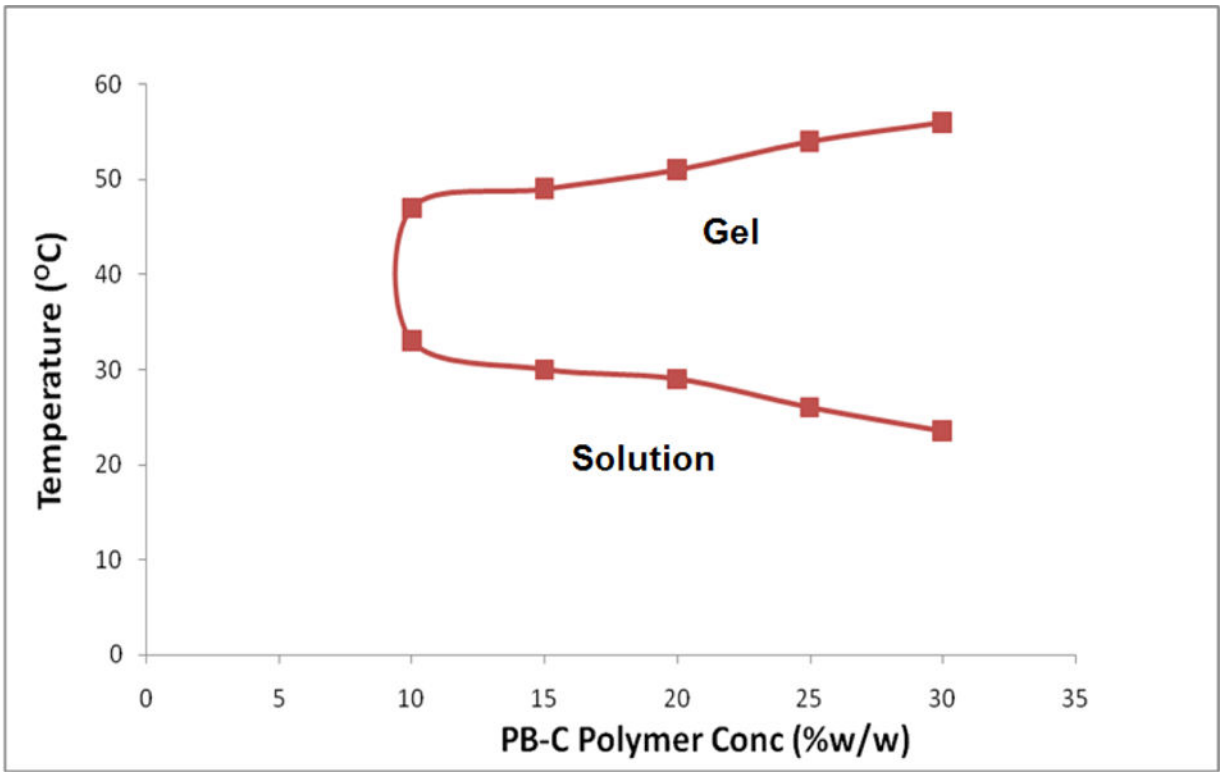

Figure 5.
Phase transition (gelation) of thermosensitive gelling copolymer PB-C

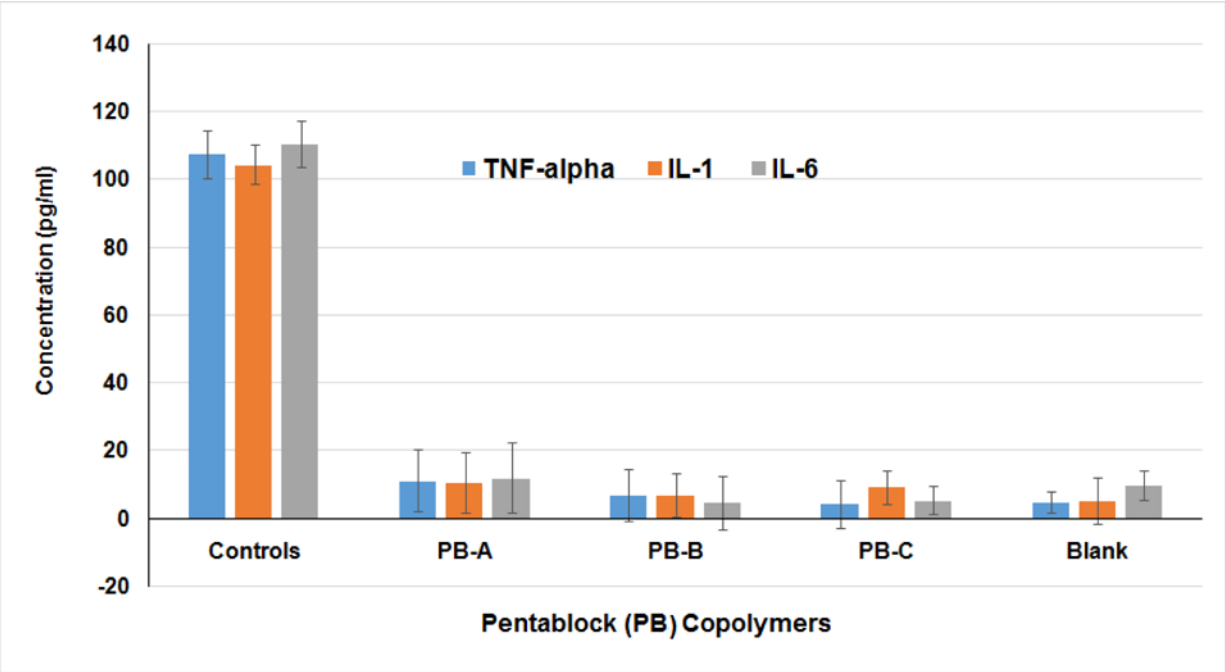

Figure 6.

In vitro biocompatibility of PB-A, PB-B and PB-C copolymers on RAW 264.7 cells estimating the levels of TNF-α, IL-6 and IL-1β in the supernatants of PB copolymers treated at 25 mg/ml.

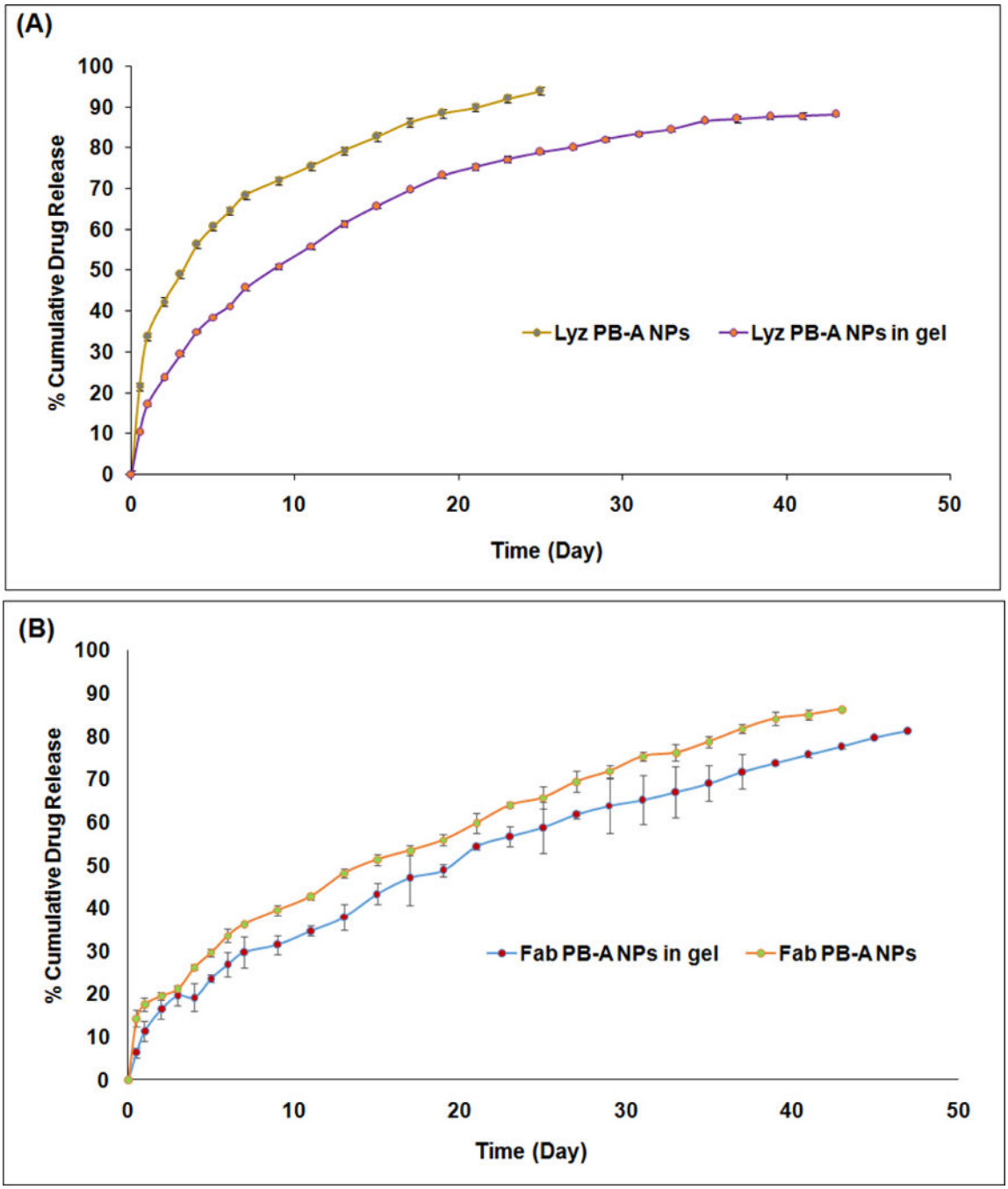

Figure 7.

(A) *In vitro* release profile of Lyz encapsulated PB-A NPs and Lyz encapsulated PB-A NPs suspended in PB-C thermosensitive gel (composite nanosystem). **(B)** *In vitro* release profile of Fab encapsulated PB-A NPs and Fab encapsulated PB-A NPs suspended in PB-C thermosensitive gel (composite nanosystem).

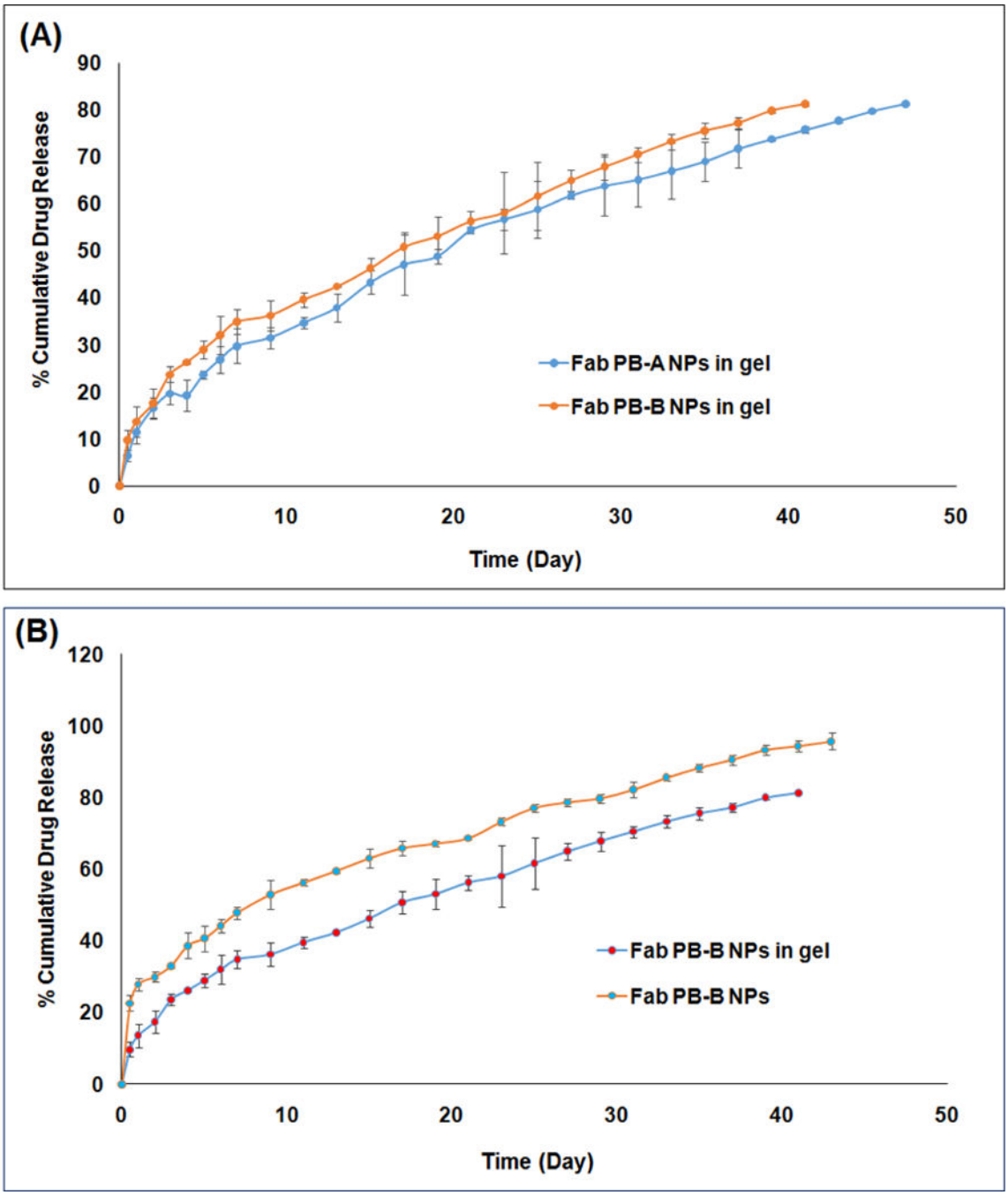

Figure 8.

(A) *In vitro* release profile of Fab encapsulated PB-A NPs and PB-B NPs suspended in PB-C thermosensitive gel (composite nanosystem). **(B)** *In vitro* release profile of Fab encapsulated PB-B NPs and PB-B NPs suspended in PB-C thermosensitive gel (composite nanosystem).

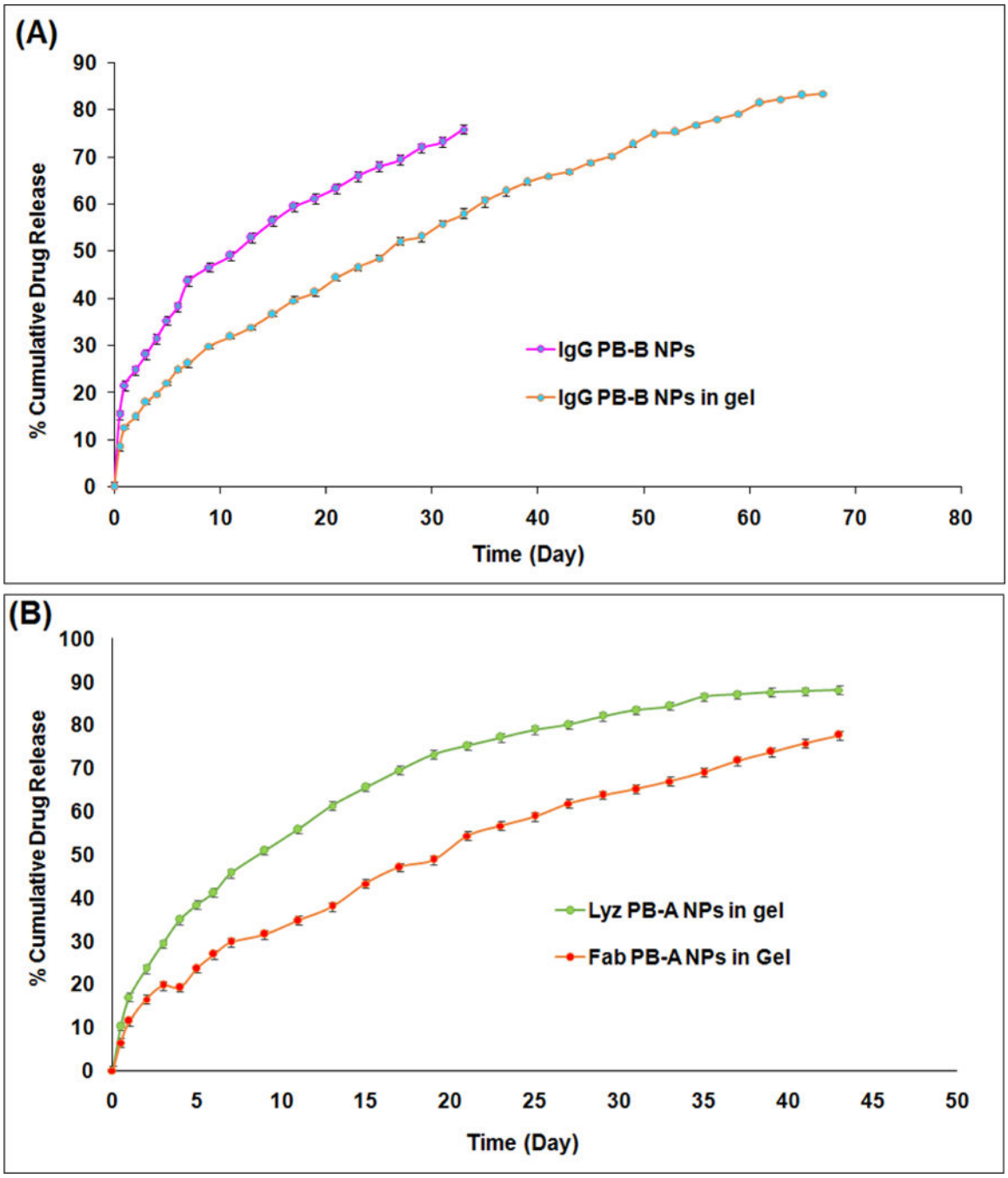

Figure 9.

(A) *In vitro* release profile of IgG encapsulated PB-B NPs and IgG encapsulated PB-B NPs suspended in PB-C thermosensitive gel (composite nanosystem). **(B)** *In vitro* release profile of Lyz or Fab encapsulated PB-A NPs suspended in PB-C thermosensitive gel (composite nanosystem).

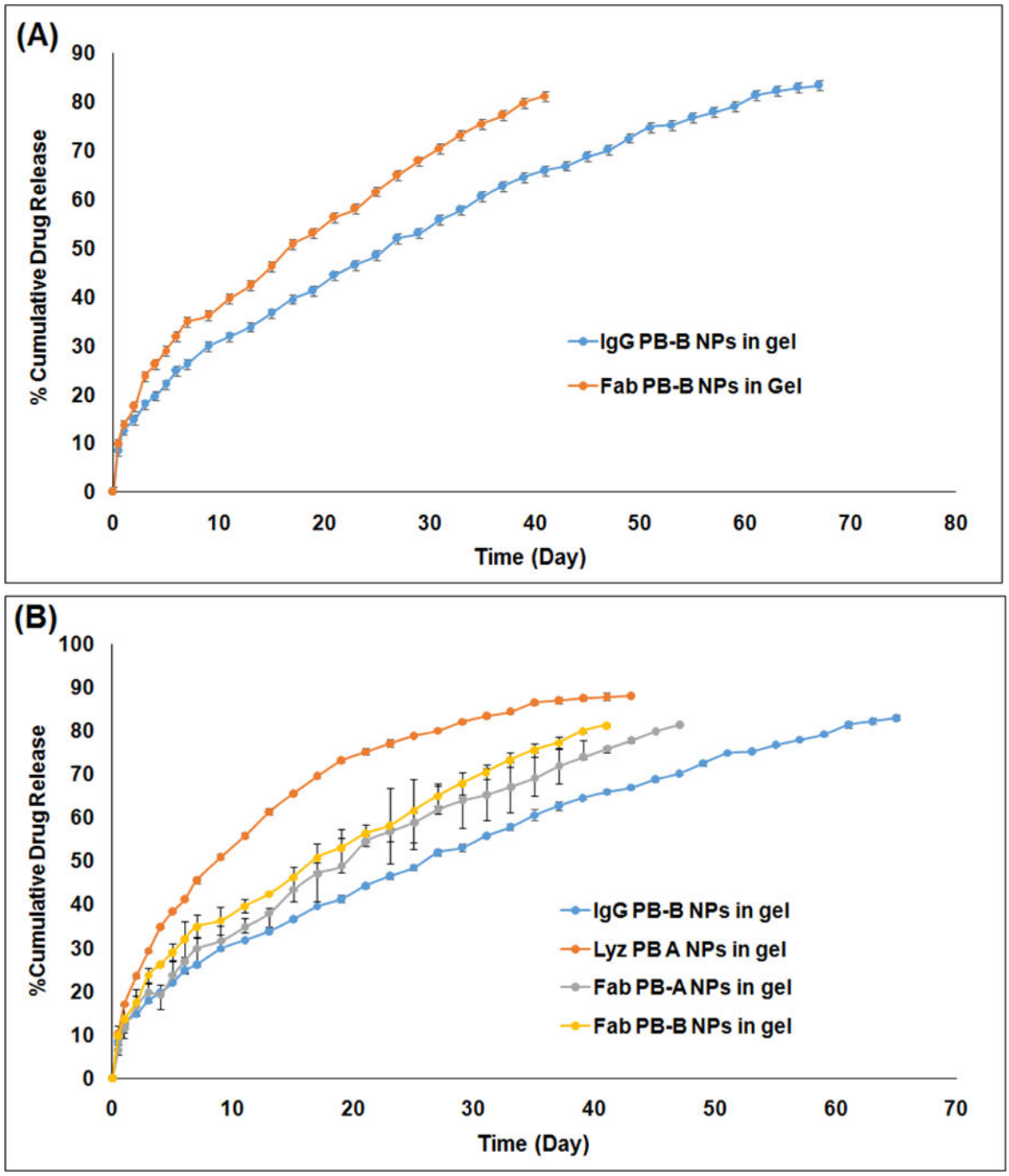

Figure 10.

(A) *In vitro* release profile of Fab or IgG encapsulated PB-B NPs suspended in PB-C thermosensitive gel (composite nanosystem). **(B)** *In vitro* release profiele of Lyz encapsulated PB-A NPS, Fab encapsulated PB-A NPs, Fab encapsulated PB-B NPs, and IgG encapsulated PB-B NPs suspended in PB-C thermosensitive gel (composite nanosystem).

Table 1

Characterization of PB copolymers

Code	Structure	Total Mn^a (theoretical)	Total Mn^b (calculated)
PB-A	PCL_{7000}-PLA_{3000}-PEG_{4000}-PLA_{3000}-PCL7000	22000	21034
PB-B	PCL_{7000}-PLA_{6000}-PEG_{4000}-PLA_{6000}-PCL7000	30000	27653
PB-C	PEG_{550}-PCL_{825}-PLA_{550}-PCL_{825}-PEG_{550}	3300	2910

[a]Theoretical value, calculated according to the feed ratio.

[b]Calculated from ^{1}H-NMR.

Table 2

Characterization of Lyz, Fab and IgG loaded PB-NPs

PB copolymers	Large molecule	Particle size (nm)	Polydispersity index (PDI)	Entrapment efficiency (% w/w) (n=3)	Loading (% w/w) (n=3)
PB-A	Lysozyme (~14.5 kDa)	221.4	0.392	42.85 ± 1.57	6.31 ± 0.79
	IgG-Fab (~50 kDa)	266.1	0.432	45.41 ± 1.30	5.46 ± 0.51
PB-B	IgG-Fab (~50 kDa)	238.5	0.398	49.28 ± 1.86	11.28 ±1.13
	IgG (~150 kDa)	201.8	0.360	51.19 ± 1.52	9.69 ± 0.46

N=3 and +/− represents the standard deviation

Table 3

Coefficient of determination (R^2) for various kinetic models for *in vitro* release of Lyz, Fab and IgG from composite nanosystems

Block copolymers	Korsmeyer-Peppas		Higuchi	First-Order	Hixon Crowell	Best fit model
	R^2	n	R^2	R^2	R^2	
Lyz NPs PB-A	0.991	0.314	0.867	0.883	0.797	Korsmeyer-Peppas
Lyz NPs PB-A suspended in thermosensitive gel	0.985	0.402	0.961	0.947	0.883	Korsmeyer-Peppas
Fab NPs PB-A	0.996	0.492	0.996	0.945	0.911	Korsmeyer-Peppas
Fab NPs PB-A suspended in thermosensitive gel	0.997	0.582	0.988	0.972	0.995	Korsmeyer-Peppas
Fab NPs PB-B	0.994	0.974	0.951	0.866	0.794	Korsmeyer-Peppas
Fab NPs PB-B suspended in thermos-sensitive gel	0.990	0.569	0.983	0.959	0. 947	Korsmeyer-Peppas
IgG NPs PB-B	0.998	0.388	0.965	0.863	0.781	Korsmeyer-Peppas
IgG NPs PB-B suspended in thermosensitive gel	0.998	0.541	0.995	0.980	0.955	Korsmeyer-Peppas

Table 4

Enzymatic activity of lysozyme estimated in the released samples

Time (days)	Specific enzyme activity (Units/mg) × 10^3	
	Release samples (n = 3)	Controls (n = 3)
1	50.3 ± 1.9	55.1 ± 3.2
7	41.2 ± 4.5	48.3 ± 3.8
14	33.6 ± 4.1	40.2 ± 4.3
21	24.5 ± 2.7	31.7 ± 3.8

N=3 and +/− represents the standard deviation